frontiers in Chemistry

ORIGINAL RESEARCH
published: 16 September 2020
doi: 10.3389/fchem.2020.00836

# Microscale Self-Assembly of Upconversion Nanoparticles Driven by Block Copolymer

*Qianqian Su*[1,2*†], *Meng-Tao Zhou*[1†], *Ming-Zhu Zhou*[1], *Qiang Sun*[3], *Taotao Ai*[4] *and Yan Su*[5*]

[1] *Institute of Nanochemistry and Nanobiology, Shanghai University, Shanghai, China,* [2] *Department of Chemistry, National University of Singapore, Singapore, Singapore,* [3] *Center for Functional Materials, NUS (Suzhou) Research Institute, Suzhou, China,* [4] *National and Local Joint Engineering Laboratory for Slag Comprehensive Utilization and Environmental Technology, School of Materials Science and Engineering, Shaanxi University of Technology, Hanzhong, China,* [5] *Genome Institute of Singapore, Agency of Science Technology and Research, Singapore, Singapore*

OPEN ACCESS

***Edited by:***
*Feng Wang,*
*City University of Hong Kong, Hong Kong*

***Reviewed by:***
*Xiaoji Xie,*
*Nanjing Tech University, China*
*Yu Wang,*
*Shenzhen University, China*

****Correspondence:***
*Qianqian Su*
*chmsqq@shu.edu.cn*
*Yan Su*
*suy1@gis.a-star.edu.sg*

*† These authors have contributed equally to this work*

***Specialty section:***
*This article was submitted to Nanoscience, a section of the journal Frontiers in Chemistry*

***Received:*** *14 July 2020*
***Accepted:*** *10 August 2020*
***Published:*** *16 September 2020*

***Citation:***
*Su Q, Zhou M-T, Zhou M-Z, Sun Q, Ai T and Su Y (2020) Microscale Self-Assembly of Upconversion Nanoparticles Driven by Block Copolymer. Front. Chem. 8:836. doi: 10.3389/fchem.2020.00836*

Lanthanide-based upconversion nanoparticles can convert low-energy excitation to high-energy emission. The self-assembled upconversion nanoparticles with unique structures have considerable promise in sensors and optical devices due to intriguing properties. However, the assembly of isotropic nanocrystals into anisotropic structures is a fundamental challenge caused by the difficulty in controlling interparticle interactions. Herein, we report a novel approach for the preparation of the chain-like assemblies of upconversion nanoparticles at different scales from nano-scale to micro-scale. The dimension of chain-like assembly can be fine-tuned using various incubation times. Our study observed Y-junction aggregate morphology due to the flexible nature of amphiphilic block copolymer. Furthermore, the prepared nanoparticle assemblies of upconversion nanoparticles with lengths up to several micrometers can serve as novel luminescent nanostructure and offer great opportunities in the fields of optical applications.

**Keywords: lanthanide-doped nanoparticles, upconversion nanoparticle, self-assembly, micro-scale, nanoparticles belt**

## INTRODUCTION

In the last decade, lanthanide-doped upconversion nanoparticles have been widely studied because of their unique optical properties including narrow emission bandwidth, large Stokes shift, long luminescence lifetime and high photostability (Auzel, 2004; Lu et al., 2013; Bettinelli et al., 2015; Li et al., 2015, 2017; Jalani et al., 2018; Liu et al., 2018; Wang et al., 2018). These nanoparticles have the potential to be used in diverse applications such as biomedicine, data storage, solar energy conversion (Chen et al., 2015, 2019; Tsang et al., 2015; Zhou B. et al., 2015; Qi et al., 2017; Su et al., 2017; Zhu et al., 2017; Chen B. et al., 2018; Chen S. et al., 2018; Gai et al., 2018; Zheng et al., 2018; Ma et al., 2019). Particularly, the growing demand of lanthanide-doped nanoparticles using in various applications has in turn greatly stimulated basic research to develop novel nanoparticles with controlled size, shape, phase and desired properties (Wang et al., 2010, 2019; Du et al., 2016; Liu D. et al., 2016; Shi et al., 2017; Kang et al., 2019; Sun et al., 2019; Wang, 2019; Wu et al., 2019; Zhao et al., 2019; Zheng et al., 2019; Chen and Wang, 2020).

The assemblies of colloidal nanoparticles with unique structure and optical properties have considerable promise in various applications (Nie et al., 2010; Singamaneni et al., 2011; Boles et al., 2016; Ariga et al., 2019; Grzelczak et al., 2019; Runowski et al., 2019). However, the assembly of isotropic nanocrystals into anisotropic structures is a fundamental challenge in nanochemistry (Liu et al., 2010; Chen and Wang, 2019). Methods have been developed for organizing inorganic nanomaterials based on inherent anisotropy of magnetic (Zhang and Wang, 2008) or electric dipoles (Si et al., 2007), external magnetic (Hu et al., 2011) or electric field-induction (Rozynek et al., 2017), spatial confinement using hard or soft templates. Specific examples of templates include linear biomacromolecules (Braun et al., 1998; Tseng et al., 2006), block copolymers (Li et al., 2011; Kim et al., 2020), carbon nanotubes (Wang et al., 2006), and so on. Despite the considerable progress made in the past several years, self-assembly of nanoparticles into an anisotropic structure is still a daunting challenge because subtle variations in interparticle interactions can cause prominent morphology changes (Su et al., 2018). Moreover, anisotropic upconversion nanoparticle self-assemblies have been rarely reported (Liu X. et al., 2016; Ren et al., 2018; Yuan et al., 2018).

Here, we report a self-assembly method of upconversion nanoparticles mediated by amphiphilic block copolymer (**Scheme 1**). This approach can obtain chain-like assemblies that span multiple length scales from nanometers to micrometers. Our study reveals a time-dependent chain-like self-assembly process. Besides, we observe Y-junction aggregate morphology due to the flexible nature of amphiphilic block copolymer. Importantly, this study provides a new route to prepare anisotropic structures materials and offer exciting opportunities for optical applications.

## MATERIALS AND METHODS

### Materials

Yttrium(III) acetate hydrate (99.9%), ytterbium(III) acetate hydrate (99.9%), thulium(III) acetate hydrate (99.9%), oleic acid (technical grade, 90%), 1-octadecene (technical grade, 90%), Igepal CO-520, tetraethyl orthosilicate (TEOS, >99.0%), ammonium fluoride (98%) sodium hydroxide (>98%), and Pluronic F127 were purchased from Sigma-Aldrich. Methanol (99.5%), cyclohexane (analytical grade), and ammonia solution (25–28%) were obtained from Aladdin. All chemicals were used as received without further purification.

### Characterization

Low-resolution transmission electron microscopy (TEM) measurements were carried out on a JEOL-JEM 2010F field emission transmission electron microscopy operated at an acceleration voltage of 200 kV. Powder X-ray diffraction (XRD) data were recorded on a Bruker D8 Advance diffractometer with a graphite monochromatized CuKα radiation (1.5406 Å). Luminescence spectra were recorded at room temperature with a DM150i monochromator equipped with an R928 photon-counting photomultiplier tube (PMT), in conjunction with a 980-nm diode laser. Upconversion luminescence microscopy imaging was performed on an Olympus BX51 microscope with the xenon lamp adapted to a diode laser. Luminescence micrographs were recorded with a Nikon DS-Ri1 imaging system. Digital photographs were taken with a Nikon D700 camera.

### Synthesis of $NaYF_4$:Yb,Tm Nanoparticles

In a typical procedure, a solution of $Ln(CH_3CO_2)_3$ (0.2 M, Ln = Y, Yb, Tm) in water (2 mL), and oleic acid (4 mL) were added to a 50 mL two-neck flask and then heated to 150°C for 30 min to remove the water content from the mixture. Then 1-octadecene (6 mL) was quickly added to the flask and the resulting mixture was maintained at 150°C for another 30 min before cooling down to 50°C. Shortly thereafter, 5 mL of a methanol solution containing $NH_4F$ (1.36 mmol) and NaOH (1 mmol) was added and the resultant mixture was stirred for 30 min at this temperature. After the methanol was evaporated, the solution was heated to 300°C under argon for 1.5 h and then cooled down to room temperature. The resulting nanoparticles were precipitated by the addition of excess ethanol, collected by centrifugation at 6,000 rpm for 5 min, and washed with ethanol several times before dispersing them in 2 mL of cyclohexane for optical and TEM measurements.

### Synthesis of $NaYF_4$:Yb,Tm$NaYF_4$ ($UCNP_{Tm}$) Nanoparticles

The as-synthesized $NaYF_4$:Yb,Tm core nanoparticles were used as seeds to epitaxial overgrowth of $NaYF_4$ layer. For the preparation of shell precursors, 0.4 mmol of $Y(CH_3CO_2)_3$ was used. The synthetic procedure is similar to the synthesis of core nanoparticles.

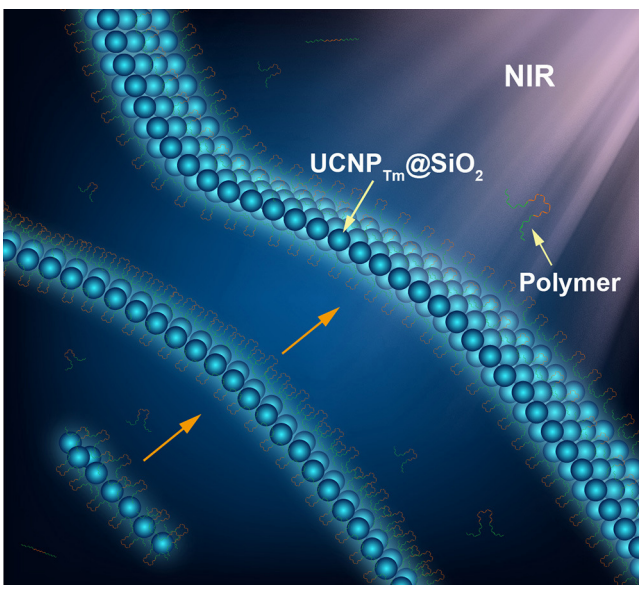


**SCHEME 1 |** Schematic illustration of amphiphilic copolymer mediated self-assembly of silica-coated upconversion nanoparticles.

## Preparation of Hydrophilic Ligand-Free $UCNP_{Tm}$ Nanoparticles

Ligand-free nanoparticles were prepared following a literature procedure (Su et al., 2012). The as-synthesized oleic acid-capped $UCNP_{Tm}$ nanoparticles were dispersed in a mixed solution of HCl (1 mL; 0.2 M) and ethanol (1 mL) and then sonicated for 5 min to remove the surface-capped ligands. The resulting ligand-free nanoparticles were centrifuged at 16,500 rpm for 20 min. The products were finally washed with ethanol and DI water several times and then re-dispersed in DI water.

## Synthesis of $NaYF_4$:Yb,Tm@$NaYF_4$@$SiO_2$ ($UCNP_{Tm}$@$SiO_2$) Nanoparticles

The synthesis of silica-coated $UCNP_{Tm}$ nanoparticles was carried out following a literature procedure (Han et al., 2017). One milliliter of Igepal CO-520 was mixed with 20 mL cyclohexane in a flask and stirred for 1 h. As-synthesized ligand-free $UCNP_{Tm}$ nanoparticles (1.5 mL) was then added into the mixture and stirred for 3 h at room temperature. After that, $NH_3 \cdot H_2O$ (150 μL, 30%) was added into the resulting mixture and stirred for another 2 h. A solution composed of TEOS (0.2 mL) and cyclohexane (0.8 mL) was introduced into the flask within 1 h by using a syringe pump. Subsequently, the mixture was hermetically stirred for 24 h at room temperature. The as-prepared products were precipitated by methanol and then centrifuged at 12,000 rpm for 10 min. The nanoparticles were then washed with a mixture of ethanol and cyclohexane three times. Finally, the nanoparticles were dispersed in deionized water.

## Self-Assembly of Upconversion Nanoparticles by F127

In a typical experiment, 100 μL $UCNP_{Tm}$@$SiO_2$ aqueous solution (1 mg $mL^{-1}$) was diluted in 3 mL DI water. 0.6 mg F127 was added to the solution and then heated to 60°C. After stirring for 1 h, the resultant suspension was incubated at 60°C for a certain time (12, 24, 48 h, and 7 days) without agitation. A few drops of nanoparticle solution were dropped onto the glass slide. Subsequently, the luminescence micrographs were captured under a recorded with a Nikon DS-Ri1 color imaging system.

# RESULTS AND DISCUSSION

## Characterization of Upconversion Nanoparticles

In terms of efficient upconversion luminescence, the inherent property of host materials and crystal nanostructure play key roles (Chen et al., 2014; Zhou J. et al., 2015). Hexagonal

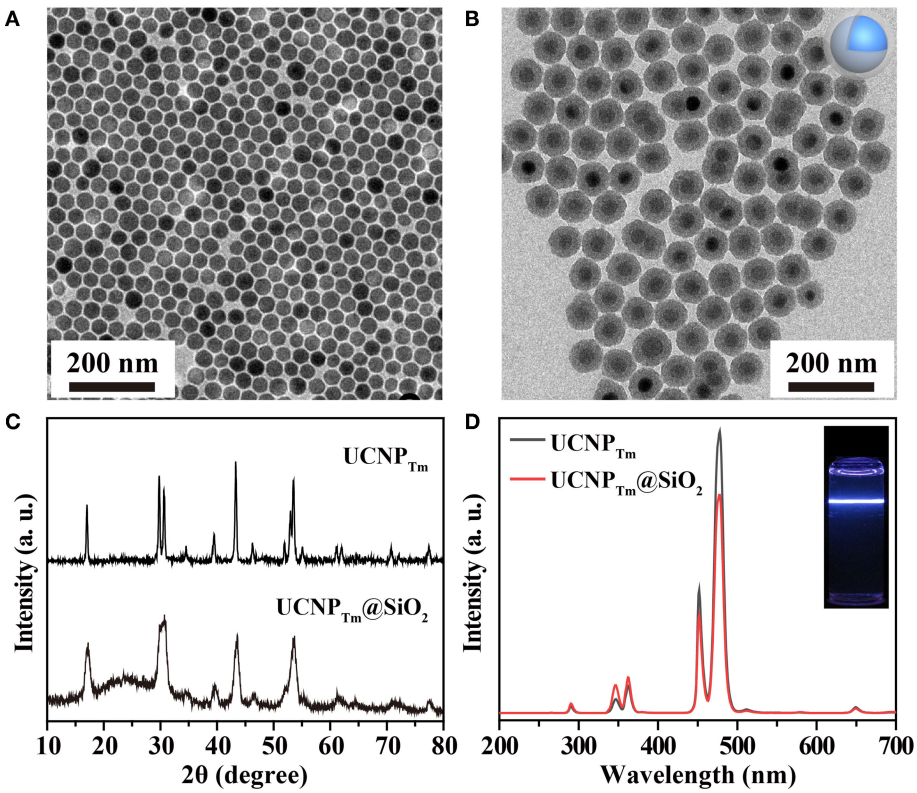


**FIGURE 1 | (A)** TEM image of $NaYF_4$:Yb,Tm nanoparticles in cyclohexane. **(B)** TEM image of $NaYF_4$:Yb,Tm@$SiO_2$ nanoparticles in water. **(C)** XRD patterns of $NaYF_4$:Yb,Tm and $NaYF_4$:Yb,Tm@$SiO_2$ nanoparticles. **(D)** The corresponding emission spectrum of the as-prepared nanoparticles and their silica-coated counterpart. Inset: luminescence photograph of $SiO_2$ coated-nanoparticles in water under irradiation of a 980 nm laser.

$NaYF_4$ is regarded as ideal host materials because of the low phonon energy and high photochemical stability (Wang et al., 2010). Additionally, optical inert $NaYF_4$ host materials can avoid unwanted energy consumption, i.e., surface quenching of the fluorescence (Su et al., 2012). Therefore, Hexagonal $NaYF_4$ was chosen as the host matrix to obtain efficient upconversion luminescence. To realize good water solubility, we coated a layer of $SiO_2$ onto the surface of upconversion nanoparticles and use them as an experimental model for the self-assembly demonstration.

We began with the synthesis of oleic acid-capped $NaYF_4$:Yb,Tm@$NaYF_4$ ($UCNP_{Tm}$) and $NaYF_4$:Yb,Er@$NaYF_4$ ($UCNP_{Er}$) core-shell nanospheres through an epitaxial growth method (Abel et al., 2009; Wang and Chen, 2019). The as-synthesized nanospheres were characterized using a transmission electron microscope (TEM). Uniform $UCNP_{Tm}$ nanoparticles

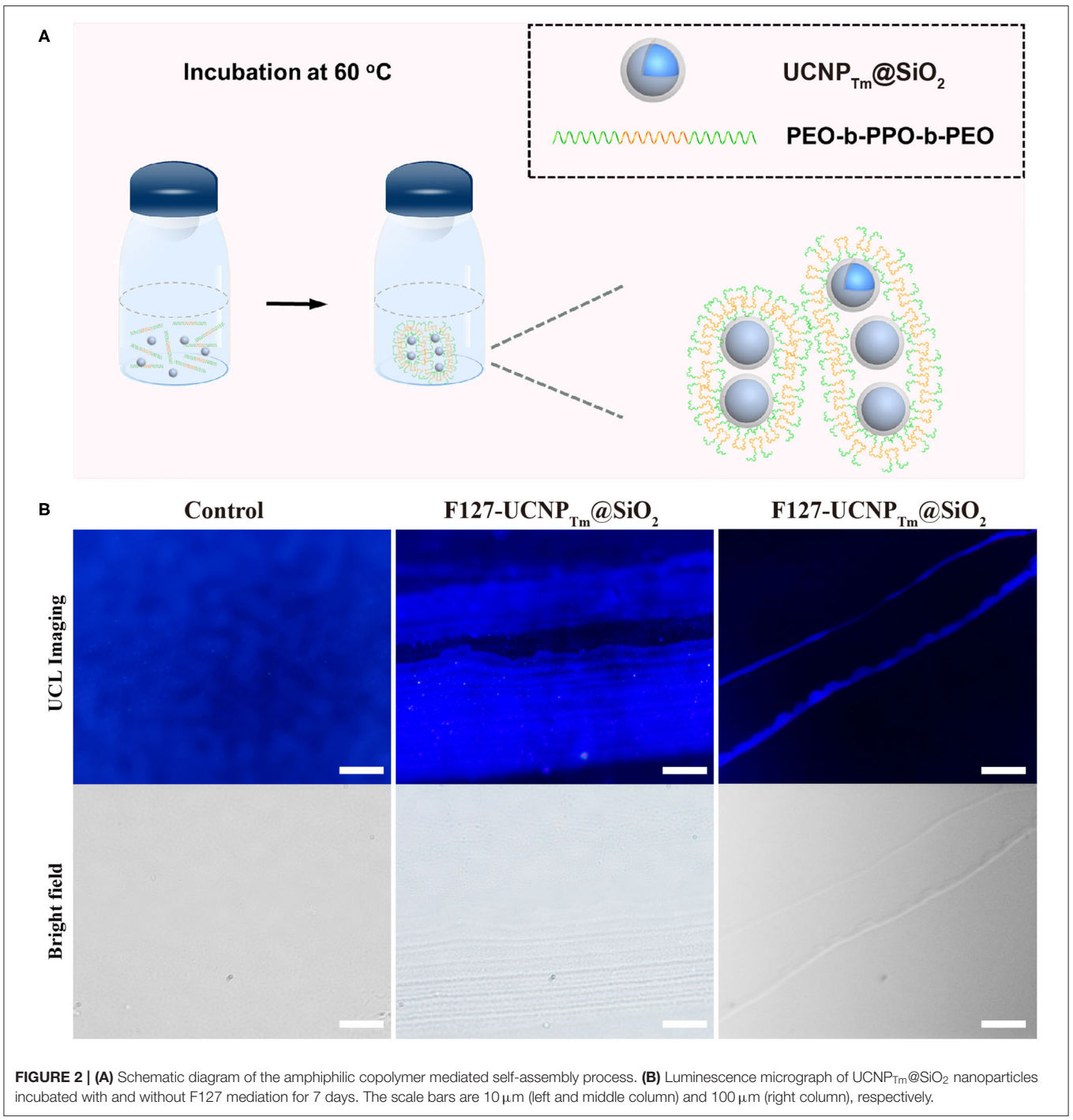


**FIGURE 2 | (A)** Schematic diagram of the amphiphilic copolymer mediated self-assembly process. **(B)** Luminescence micrograph of $UCNP_{Tm}$@$SiO_2$ nanoparticles incubated with and without F127 mediation for 7 days. The scale bars are 10 μm (left and middle column) and 100 μm (right column), respectively.

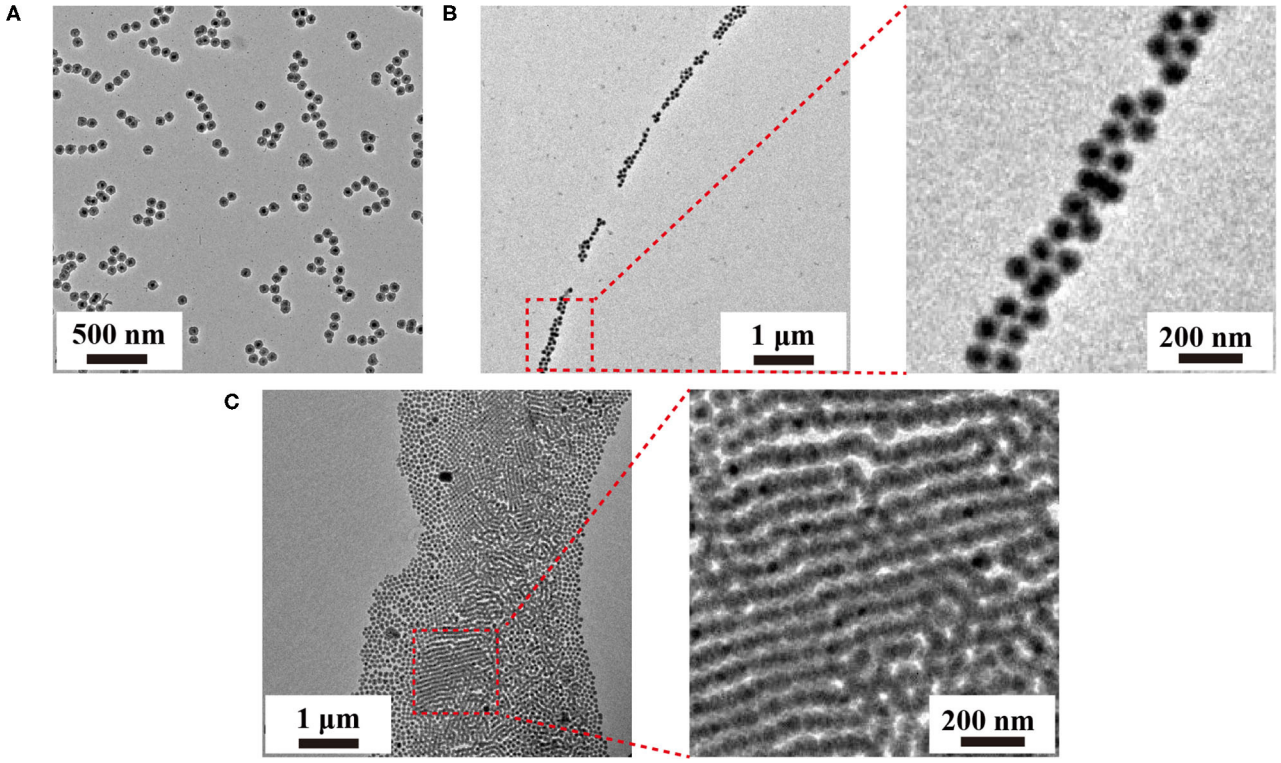


**FIGURE 3 |** TEM images of the as-prepared upconversion nanoparticle assemblies mediated by F127 under varied incubation time, 12 h **(A)**, 24 h, **(B)**, 48 h **(C)**, respectively.

with an average diameter of about 36 nm for $UCNP_{Tm}$ were obtained and shown in **Figure 1A** and **Supplementary Figure 1**. After silica coating on the surface of $UCNP_{Tm}$ nanospheres, the size of the nanoparticles reached about 76 nm (**Figure 1B** and **Supplementary Figure 2**). The dynamic light scattering (DLS) measurement show that the hydrodiameter of $UCNP_{Tm}@SiO_2$ nanoparticles was around 90 nm (PDI = 0.13), demonstrating their mono-dispersion in water (**Supplementary Figure 3**). X-ray powder diffraction (XRD) analysis was conducted to confirm the phase-purity of $UCNP_{Tm}$ nanoparticles, which can be indexed as a hexagonal phase of $NaYF_4$ (JCPDS file number 16-0334) (**Figure 1C**). A broad diffraction peak at $2\theta = 22^{\circ}$ appeared in $UCNP_{Tm}@SiO_2$ nanoparticles pattern, which can be ascribed to the peak of amorphous silica (Zhou et al., 2019).

We next studied the optical properties of as-prepared upconversion nanoparticles. Upon 980 nm excitation, $Tm^{3+}$ ions in $UCNP_{Tm}$ nanoparticles exhibit a characteristic emission at 290 nm ($^1I_6 \rightarrow {}^3H_6$), 345 nm ($^1I_6 \rightarrow {}^3H_5$), 360 nm ($^1D_2 \rightarrow {}^3H_6$), 450 nm ($^1D_2 \rightarrow {}^3F_4$), 475 nm ($^1G_4 \rightarrow {}^3H_6$), 511 nm ($^1D_2 \rightarrow {}^3H_5$) and 650 nm ($^1G_4 \rightarrow {}^3F_4$) from ultraviolent to visible region (Wang and Liu, 2008), respectively (**Figure 1D**). After silica coating, the luminescent intensity was slightly weaker compared to oleic acid-coated nanoparticles. The resulting nanoparticles were dispersed in DI water prior to being used for self-assembly demonstration (**Figure 1D**, inset).

As a proof-of-concept experiment, the amphiphilic copolymer F127 was employed as a surfactant to mediate the self-assembly process of $UCNP_{Tm}@SiO_2$ nanoparticles. The procedure the $UCNP_{Tm}@SiO_2$ nanoparticles self-assembly was shown in **Figure 2A**. In a typical experiment, we simply mixed $UCNP_{Tm}@SiO_2$ and amphiphilic copolymer F127 in aqueous solution and then heated to 60°C. Upon aging the nanoparticles in amphiphilic copolymer aqueous solution for 7 days without agitation, upconversion nanoparticles long belts gradually generated. As shown in **Figure 2B** (middle and right column), long upconversion nanoparticles belts composed by horizontally arranged nanoparticle chains were clearly observed and the nanoparticle belts reach to micro-scale. However, we didn't observe any organized structure without the addition of copolymer F127 (**Figure 2B**, left column). To our knowledge, this is the first observation of a micrometer scale upconversion nanoparticles belts by solution self-assembly of amphiphilic block copolymers.

The formation of the upconversion nanoparticle chains was then studied using TEM as shown in **Figure 3A**. The nanoparticles connected in a one-dimensional tendency upon short incubation time (12 h) with amphiphilic copolymer F127. TEM images revealed the presence of the short chains composed by several to a dozen nanoparticles. The interparticle separations between $UCNP_{Tm}@SiO_2$ nanoparticles in the chain

were observed (**Supplementary Figure 4**), indicating that the obtained nanoparticle chains are connected by the molecular linker. Noted that hot water can etch away the $SiO_2$ shell by breaking the internal Si-O-Si bonds (Liu et al., 2014). Our nanoparticles were slightly etched due to the protection of F127 copolymer. When the incubation time was prolonged to 24 h, we observed long chains of $UCNP_{Tm}@SiO_2$ nanoparticles which reached microscale in length (**Figure 3B**). The nanoparticles

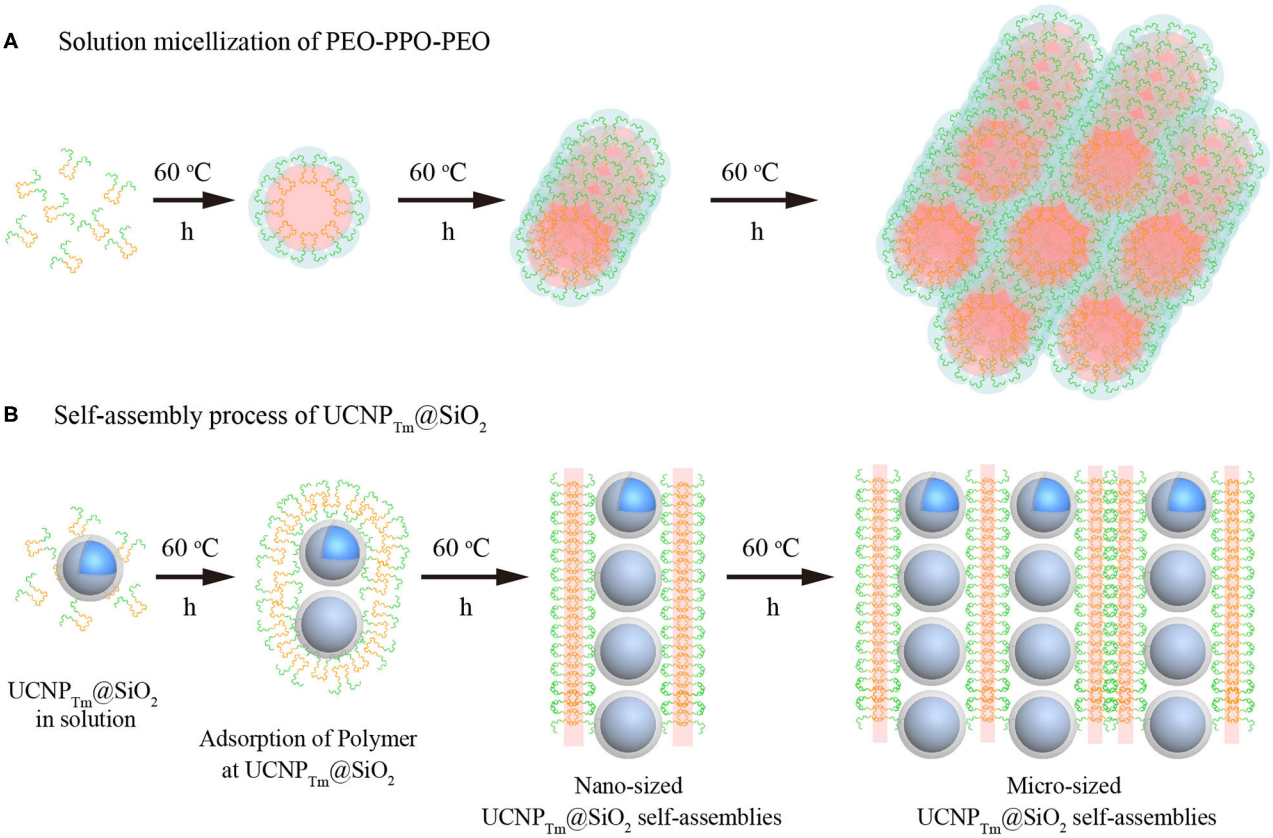


**FIGURE 4 | (A)** Morphological transitions of amphiphilic block copolymers F127 as a function of time. **(B)** Schematic illustration of the self-assembly process for $SiO_2$-coated upconversion nanoparticles. Note that the green chain denotes hydrophilic segment PEO, and the orange chain represents hydrophobic segment PPO of F127, respectively.

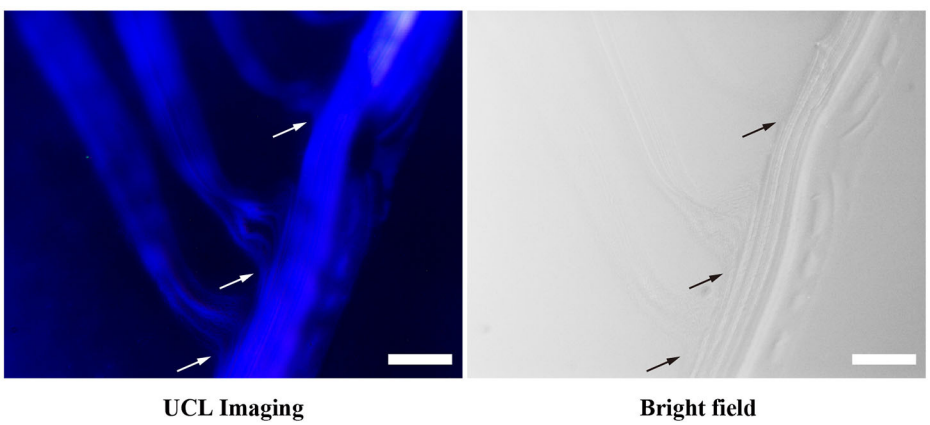


**FIGURE 5 |** Luminescence micrograph demonstrates the existence of Y-junctions of $UCNP_{Tm}@SiO_2$ assemblies incubated with F127 mediation for 7 days. Arrows indicate examples of Y-junctions. The scale bars are 10 μm.

chains have an average width of 1–3 nanoparticles. Interestingly, further prolonging the incubation time resulted in the formation of upconversion nanoparticle belts. As shown in **Figure 3C**, TEM images revealed the presence of the belts with an average belt length of 40–50 nanoparticles and as wide as about 2.5–4 μm. Furthermore, these nanoparticles under the drive of interfacial energy would spontaneously assemble in close-packed arrangements during the extended incubation period. This result is also consistent with the luminescence micrographs of $UCNP_{Tm}@SiO_2$ nanoparticle showing horizontally arranged nanoparticle chains. By contrast, we observe a random pattern of $UCNP_{Tm}@SiO_2$ nanoparticles without the addition of copolymer F127 (**Supplementary Figure 5**).

The ability of amphiphilic block copolymers to drive $UCNP_{Tm}@SiO_2$ nanoparticles self-assemble into chain-like nanostructures when dissolved in water is based on the specific amphiphilic character of this block copolymer F127. These amphiphilic block copolymers consist of a polar, hydrophilic polymer block (PEO) and a non-polar, lipophilic polymer block (PPO). In water, which is a thermodynamically good solvent for the PEO block but a poor solvent for the PPO block, the "insoluble" PPO block aggregates and forms a core while the "soluble" PEO block forms a corona that interacts with the water and stabilizes the polymer self-assembly (Alexandridis et al., 1994; Liu and Li, 2015). As shown in **Figure 4A**, the formation of one-dimensional chains may be induced by the transition from spherical to long cylindrical micelles of the amphiphilic block copolymer. It should be noted that the self-assembly of amphiphilic block copolymers in specific block-selective solvents generates morphologies such as spheres, cylindrical micelles, and a variety of other architectures (Kang et al., 2005; Gilroy et al., 2010).

$SiO_2$ coated upconversion nanoparticles exhibited durable super-hydrophilic surface properties due to that the surface of silica particles is covered with SiOH groups. The PEO-PPO-PEO block copolymer can be absorbed on the hydrophilic surfaces. On hydrophilic surfaces, these block copolymer surfactants adsorb with their hydrophilic tail (PEO) toward the $SiO_2$ surface, resulting in double-layer adsorption (Malmsten et al., 1992). Furthermore, when the incubation time was prolonged, the size of the cylindrical micelles became larger in width and length, and thus micro-scaled nanoparticle assembly was formed (**Figure 4B**). It should be noted that our results are also consistent with the previous experimental evidence showing that the length of cylindrical block copolymer micelles could reach up to ∼200 nm to 2 μm (Gilroy et al., 2010). Taken together, we suggest that $UCNP_{Tm}@SiO_2$ nanoparticles prefer to assemble in a chain manner might be caused by the mutual attraction between the hydrophilic-hydrophilic interactions (Fukao et al., 2009) and cylindrical micelles formed by the self-assembly process of block copolymers F127.

In addition to chain-like assemblies spanning from the nanometer to the micrometer length scale, we also observed occasional Y-junctions of $UCNP_{Tm}@SiO_2$ assemblies incubated with F127 mediation for 7 days by using the luminescence microscope and the image was shown in **Figure 5**. To further demonstrate the existence of Y-junctions, we carefully examined the 24 h-incubation samples of $UCNP_{Tm}@SiO_2$ by TEM image.

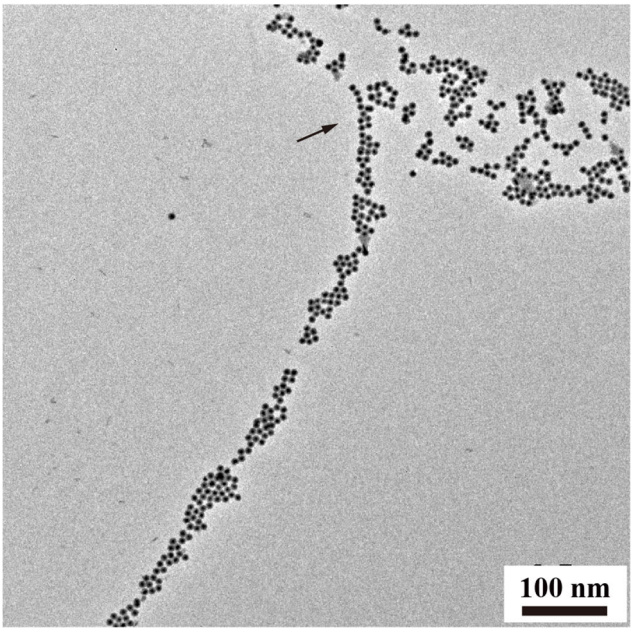


**FIGURE 6 |** TEM analysis of Y-junctions of $UCNP_{Tm}@SiO_2$ assemblies incubated with F127 mediation for 24 h. Arrows indicate examples of Y-junctions.

As expected, we observed the formation of Y-junctions, and TEM images were shown in **Figure 6**. This morphology may be ascribed to typical structural defects associated with the formation of the cylindrical micelle (Fenyves et al., 2014). It was reported that the formation of structural defects (i.e., Y-junctions) becomes prevalent when micellization kinetics slow down (Tlusty and Safran, 2000). We observed some Y-junctions (**Supplementary Figure 6**). We hypothesized that such a behavior can be ascribed to the flexible nature of F127 copolymer, which can accommodate packing frustrations in structures that have significant deviations from the mean curvature. This explanation was consistent with the previous report indicating that the packing frustrations associated with deviations from the mean curvature in the Y-junctions would be alleviated by chain stretching of polymers with high molecular weight (Jain and Bates, 2003). Moreover, our mechanism is different from the DNA mediated self-assembly mechanism reported by Jin and coworkers, which involves anisotropic surface functionalization of upconversion nanoparticle that directs the anisotropic pattern of upconversion nanoparticle self-assembly (Ren et al., 2018).

## CONCLUSIONS

In conclusion, we have presented a novel approach for controlling the one-dimensional assemblies of upconversion nanoparticles at different scales from nano-scale to micro-scale. The results revealed time-dependent morphology, producing chain-like and belt-like structures. Our study suggests that the morphology is depending on the morphology of micelles of amphiphilic block copolymers in specific conditions. And the

driving force for the self-assembly of upconversion nanoparticles is particle surface hydrophobic and hydrophilic force offered by amphiphilic polymers. Furthermore, this work may lead to new applications for upconversion nanoparticles and may provide insightful ideas for the design of other functional nanomaterials.

## DATA AVAILABILITY STATEMENT

All datasets generated for this study are included in the article/**Supplementary Material**.

## AUTHOR CONTRIBUTIONS

QSu and YS conceived the project. QSu, M-TZ, YS, M-ZZ, and QSun were primarily responsible for the experiments of nanoparticle synthesis and characterization. QSu, M-TZ, YS, and TA contributed to the data analyses and discussion. QSu, YS, and TA prepared figures and wrote the paper with input from other authors. All authors contributed to the article and approved the submitted version.

## ACKNOWLEDGMENTS

We are thankful for financial support from the National Natural Science Foundation of China (Nos. 21701109 and 21701119) and the National Basic Research Program of China (No. 2016YFA0201600). The content of this manuscript has been published in part as part of the thesis of Su Qianqian (Su, 2013).

## SUPPLEMENTARY MATERIAL

The Supplementary Material for this article can be found online at: https://www.frontiersin.org/articles/10.3389/fchem.2020.00836/full#supplementary-material

## REFERENCES

Abel, K. A., Boyer, J. C., and van Veggel, F. C. J. M. (2009). Hard proof of the $NaYF_4$/$NaGdF_4$ nanocrystal core/shell structure. *J. Am. Chem. Soc.* 131, 14644–14645. doi: 10.1021/ja906971y

Alexandridis, P., Holzwarth, J. F., and Hatton, T. A. (1994). Micellization of poly(ethylene oxide)-poly(propylene oxide)-poly(ethylene oxide) triblock copolymers in aqueous solutions: thermodynamics of copolymer association. *Macromolecules* 27, 2414–2425. doi: 10.1021/ma00087a009

Ariga, K., Nishikawa, M., Mori, T., Takeya, J., Shrestha, L. K., and Hill, J. P. (2019). Self-assembly as a key player for materials nanoarchitectonics. *Sci. Technol. Adv. Mater.* 20, 51–95. doi: 10.1080/14686996.2018.1553108

Auzel, F. (2004). Upconversion and anti-Stokes processes with f and d ions in solids. *Chem. Rev.* 104, 139–173. doi: 10.1021/cr020357g

Bettinelli, M., Carlos, L. D., and Liu, X. (2015). Lanthanide-doped upconversion nanoparticles. *Phys. Today* 68, 38–44. doi: 10.1063/PT.3.2913

Boles, M. A., Engel, M., and Talapin, D. V. (2016). Self-assembly of colloidal nanocrystals: from intricate structures to functional materials. *Chem. Rev.* 116, 11220–11289. doi: 10.1021/acs.chemrev.6b00196

Braun, E., Eichen, E., Sivan, U., and Ben-Yoseph, G. (1998). DNA-templated assembly and electrode attachment of a conducting silver wire. *Nature* 391, 775–778. doi: 10.1038/35826

Chen, B., Su, Q., Kong, W., Wang, Y., Shi, P., and Wang, F. (2018). Energy transfer-based biodetection using optical nanomaterials. *J. Mater. Chem. B* 6, 2924–2944. doi: 10.1039/c8tb00614h

Chen, B., and Wang, F. (2019). Combating concentration quenching in upconversion nanoparticles. *Acc. Chem. Res.* 53, 358–367. doi: 10.1021/acs.accounts.9b00453

Chen, B., and Wang, F. (2020). Emerging frontiers of upconversion nanoparticles. *Trends Chem.* 2, 427. doi: 10.1016/j.trechm.2020.01.008

Chen, G., Agren, H., Ohulchanskyy, T. Y., and Prasad, P. N. (2015). Light upconverting core-shell nanostructures: nanophotonic control for emerging applications. *Chem. Soc. Rev.* 44, 1680–1713. doi: 10.1039/c4cs00170b

Chen, G., Qiu, H., Prasad, P. N., and Chen, X. (2014). Upconversion nanoparticles: design, nanochemistry, and applications in theranostics. *Chem. Rev.* 114, 5161–5214. doi: 10.1021/cr400425h

Chen, L., Su, B., and Jiang, L. (2019). Recent advances in one-dimensional assembly of nanoparticles. *Chem. Soc. Rev.* 48, 8–21. doi: 10.1039/c8cs00703a

Chen, S., Weitemier, A. Z., Zeng, X., He, L., Wang, X., Tao, Y., et al. (2018). Near-infrared deep brain stimulation via upconversion nanoparticle-mediated optogenetics. *Science* 359, 679–683. doi: 10.1126/science.aaq1144

Du, P., Luo, L., Park, H. K., and Yu, J. S. (2016). Citric-assisted sol-gel based $Er3^+$/$Yb^{3+}$-codoped $Na_{0.5}Gd_{0.5}MoO_4$: A novel highly-efficient infrared-to-visible upconversion material for optical temperature sensors and optical heaters. *Chem. Eng. J.* 306, 840–848. doi: 10.1016/j.cej.2016.08.007

Fenyves, R., Schmutz, M., Horner, I. J., Bright, F. V., and Rzayev, J. (2014). Aqueous self-assembly of giant bottlebrush block copolymer surfactants as shape-tunable building blocks. *J. Am. Chem. Soc.* 136, 7762–7770. doi: 10.1021/ja503283r

Fukao, M., Sugawara, A., Shimojima, A., Fan, W., Arunagirinathan, M. A., Tsapatsis, M., et al. (2009). One-dimensional assembly of silica nanospheres mediated by block copolymer in liquid phase. *J. Am. Chem. Soc.* 131:16344. doi: 10.1021/ja907013u

Gai, S., Yang, G., Yang, P., He, F., Lin, J., Jin, D., et al. (2018). Recent advances in functional nanomaterials for light-triggered cancer therapy. *Nano Today* 19, 146–187. doi: 10.1016/j.nantod.2018.02.010

Gilroy, J. B., Gadt, T., Whittell, G. R., Chabanne, L., Mitchels, J. M., Richardson, R. M., et al. (2010). Monodisperse cylindrical micelles by crystallization-driven living self-assembly. *Nat. Chem.* 2, 566–570. doi: 10.1038/nchem.664

Grzelczak, M., Liz-Marzan, L. M., and Klajn, R. (2019). Stimuli-responsive self-assembly of nanoparticles. *Chem. Soc. Rev.* 48, 1342–1361. doi: 10.1039/c8cs00787j

Han, S., Samanta, A., Xie, X., Huang, L., Peng, J., Park, S. J., et al. (2017). Gold and hairpin DNA functionalization of upconversion nanocrystals for imaging and in vivo drug delivery. *Adv. Mater.* 29:1700244. doi: 10.1002/adma.201700244

Hu, Y., He, L., and Yin, D. (2011). Magnetically responsive photonic nanochains. *Angew. Chem. Int. Ed.* 50, 3747–3750. doi: 10.1002/anie.201100290

Jain, S., and Bates, F. S. (2003). On the origins of morphological complexity in block copolymer surfactants. *Science* 300, 460–464. doi: 10.1126/science.1082193

Jalani, G., Tam, V., Vetrone, F., and Cerruti, M. (2018). Seeing, targeting and delivering with upconverting nanoparticles. *J. Am. Chem. Soc.* 140, 10923–10931. doi: 10.1021/jacs.8b03977

Kang, M., Kang, H., Park, S., and Jang, H. S. (2019). Facile synthesis of sub-10 nm-sized bright red-emitting upconversion nanophosphors via tetrahedral YOF: Yb, Er seed-mediated growth. *Chem. Commun.* 55, 13350–13353. doi: 10.1039/c9cc06797c

Kang, Y., Erickson, K. J., and Taton, T. A. (2005). Plasmonic nanoparticle chains via a morphological, sphere-to-string transition. *J. Am. Chem. Soc.* 127, 13800–13801. doi: 10.1021/ja055090s

Kim, J. H., Jin, H. M., Yang, G. G., Han, K. H., Yun, T., Shin, J. Y., et al. (2020). Smart nanostructured materials based on self-assembly of block copolymers. *Adv. Funct. Mater.* 30:1902049. doi: 10.1002/adfm.201902049

Li, W., Liu, S., Deng, R., and Zhu, J. (2011). Encapsulation of nanoparticles in block copolymer micellar aggregates by directed supramolecular assembly. *Angew. Chem. Int. Ed.* 50, 5865–5868. doi: 10.1002/anie.201008224

Li, X., Zhang, F., and Zhao, D. (2015). Lab on upconversion nanoparticles: optical properties and applications engineering via designed nanostructure. *Chem. Soc. Rev.* 44, 1346–1378. doi: 10.1039/c4cs00163j

Li, Z., Yuan, H., Yuan, W., Su, Q., and Li, F. (2017). Upconversion nanoprobes for biodetections. *Coord. Chem. Rev.* 354, 155–168. doi: 10.1016/j.ccr.2017.06.025

Liu, D., Xu, X., Du, Y., Qin, X., Zhang, Y., Ma, C., et al. (2016). Three-dimensional controlled growth of monodisperse sub-50 nm heterogeneous nanocrystals. *Nat. Commun.* 7, 10254. doi: 10.1038/ncomms10254

Liu, J., Bu, J., Bu, W., Zhang, S., Pan, L., Fan, W., et al. (2014). Real-time in vivo quantitative monitoring of drug release by dual-mode magnetic resonance and upconverted luminescence imaging. *Angew. Chem. Int. Ed.* 53, 4551–4555. doi: 10.1002/anie.201400900

Liu, K., Nie, Z., Zhao, N., Li, W., Rubinstein, M., and Kumacheva, E. (2010). Step-growth polymerization of inorganic nanoparticles. *Science* 329, 197–200. doi: 10.1126/science.1189457

Liu, L., Wang, S., Zhao, B., Pei, P., Fan, Y., Li, X., et al. (2018). $Er^{3+}$ sensitized 1530 nm to 1180 nm second near-infrared window upconversion nanocrystals for in vivo biosensing. *Angew. Chem. Int. Ed.* 57, 7518–7522. doi: 10.1002/anie.201802889

Liu, S., and Li, L. (2015). Molecular interactions between PEO-PPO-PEO and PPO-PEO-PPO triblock copolymers in aqueous solution. *Colloid Surf. A Physicochem. Eng. Asp.* 484, 485–497. doi: 10.1016/j.colsurfa.2015.08.034

Liu, X., Ni, Y., Zhu, C., Fang, L., Kou, J., Lu, C., et al. (2016). Controllable self-assembly of $NaREF_4$ upconversion nanoparticles and their distinctive fluorescence properties. *Nanotechnology* 27:295605. doi: 10.1088/0957–4484/27/29/295605

Lu, Y., Zhao, J., Zhang, R., Liu, Y., Liu, D., Goldys, E. M., et al. (2013). Tunable lifetime multiplexing using luminescent nanocrystals. *Nat. Photonics* 8, 33–37. doi: 10.1038/nphoton.2013.322

Ma, Y., Bao, J., Zhang, Y., Li, Z., Zhou, X., Wan, C., et al. (2019). Mammalian near-infrared image vision through injectable and self-powered retinal nanoantennae. *Cell* 177, 243. doi: 10.1016/j.cell.2019.01.038

Malmsten, M., Linse, P., and Cosgrove, T. (1992). Adsorption of PEO-PPO-PEO block copolymers at silica. *Macromolecules* 25, 2474–2481.

Nie, Z., Petukhova, A., and Kumacheva, E. (2010). Properties and emerging applications of self-assembled structures made from inorganic nanoparticles. *Nat. Nanotechnol.* 5, 15–25. doi: 10.1038/nnano.2009.453

Qi, Q., Li, C., Liu, X., Jiang, S., Xu, Z., Lee, R., et al. (2017). Solid-state photoinduced luminescence switch for advanced anticounterfeiting and super-resolution imaging applications. *J. Am. Chem. Soc.* 139, 16036–16039. doi: 10.1021/jacs.7b07738

Ren, W., Wen, S., Tawfik, S. A., Lin, G., Ford, M. J., Jin, D., et al. (2018). Anisotropic functionalization of upconversion nanoparticles. *Chem. Sci.* 9, 4352–4358. doi: 10.1039/c8sc01023d

Rozynek, Z., Han, M., Dutka, F., Garstecki, P., Jozefczak, A., and Luijten, E. (2017). Formation of printable granular and colloidal chains through capillary effects and dielectrophoresis. *Nat. Commun.* 8:15255. doi: 10.1038/ncomms15255

Runowski, M., Stopikowska, N., Szeremeta, D., Goderski, S., Skwierczynska, M., and Lis, S. (2019). Upconverting lanthanide fluoride core@shell nanorods for luminescent thermometry in the first and second biological windows: beta-$NaYF_4$: $Yb^{3+}$-$Er^{3+}$@$SiO_2$ temperature sensor. *ACS Appl. Mater. Interfaces* 11, 13389–13396. doi: 10.1021/acsami.9b00445

Shi, R., Ling, X., Li, X., Zhang, L., Lu, M., Xie, X., et al. (2017). Tuning hexagonal $NaYbF_4$ nanocrystals down to sub-10 nm for enhanced photon upconversion. *Nanoscale* 9, 13739–13746. doi: 10.1039/c7nr04877g

Si, S., Kotal, A., and Mandal, T. K. (2007). One-dimensional assembly of peptide-functionalized gold nanoparticles: an approach toward mercury ion sensing. *J. Phys. Chem. C* 111, 1248–1255. doi: 10.1021/jp066303i

Singamaneni, S., Bliznyuk, V. N., Binek, C., and Tsymbal, E. Y. (2011). Magnetic nanoparticles: recent advances in synthesis, self-assembly and applications. *J. Mater. Chem.* 21, 16819–16845. doi: 10.1039/c1jm11845e

Su, Q. (2013). *Luminescent Nanocrystals: Synthesis, Characterization and Optical Tuning*. [Ph.D. thesis]. [Singapore]: National University of Singapore.

Su, Q., Feng, W., Yang, D., and Li, F. (2017). Resonance energy transfer in upconversion nanoplatforms for selective biodetection. *Acc. Chem. Res.* 50, 32–40. doi: 10.1021/acs.accounts.6b00382

Su, Q., Han, S., Xie, X., Zhu, H., Chen, H., Chen, C., et al. (2012). The effect of surface coating on energy migration-mediated upconversion. *J. Am. Chem. Soc.* 134, 20849–20857. doi: 10.1021/ja3111048

Su, Q., Zou, R., Su, Y., and Fan, S. (2018). Morphology control and growth mechanism study of quantum-sized ZnS nanocrystals from single-source precursors. *J. Nanosci. Nanotechnol.* 18:6850. doi: 10.1166/jnn.2018.15516

Sun, T., Li, Y., Ho, W. L., Zhu, Q., Chen, X., Jin, L., et al. (2019). Integrating temporal and spatial control of electronic transitions for bright multiphoton upconversion. *Nat. Commun.* 10:1811. doi: 10.1038/s41467-019-09850-2

Tlusty, T., and Safran, S. A. (2000). Microemulsion networks: the onset of bicontinuity. *J. Phys.: Condens. Matter* 12, A253–A262. doi: 10.1088/0953-8984/12/8a/332

Tsang, M. K., Bai, G., and Hao, J. (2015). Stimuli responsive upconversion luminescence nanomaterials and films for various applications. *Chem. Soc. Rev.* 44, 1585–1607. doi: 10.1039/c4cs00171k

Tseng, R. J., Tsai, C. L., Ma, L. P., and Ouyang, J. Y. (2006). Digital memory device based on tobacco mosaic virus conjugated with nanoparticles. *Nat. Nanotechnol.* 1, 72–77. doi: 10.1038/nnano.2006.55

Wang, D., Li, Z. C., and Chen, L. (2006). Templated synthesis of single-walled carbon nanotube and metal nanoparticle assemblies in solution. *J. Am. Chem. Soc.* 128, 15078–15079. doi: 10.1021/ja066617j

Wang, F., Han, Y., Lim, C. S., Lu, Y., Wang, J., Xu, J., et al. (2010). Simultaneous phase and size control of upconversion nanocrystals through lanthanide doping. *Nature* 463, 1061–1065. doi: 10.1038/nature08777

Wang, F., and Liu, X. (2008). Upconversion multicolor fine-tuning:visible to near-infrared emission from lanthanide-doped $NaYF_4$ nanoparticles. *J. Am. Chem. Soc.* 130:5642. doi: 10.1021/ja800868a

Wang, S., Shen, B., Wei, H. L., Liu, Z., Chen, Z., Zhang, Y., et al. (2019). Comparative investigation of the optical spectroscopic and thermal effect in $Nd^{3+}$-doped nanoparticles. *Nanoscale* 11, 10220–10228. doi: 10.1039/c9nr02493j

Wang, X., and Chen, G. (2019). A strategy for prompt phase transfer of upconverting nanoparticles through surface oleate-mediated supramolecular assembly of amino-beta-cyclodextrin. *Front. Chem.* 7:161. doi: 10.3389/fchem.2019.00161

Wang, Y. (2019). The role of an inert shell in improving energy utilization in lanthanide-doped upconversion nanoparticles. *Nanoscale* 11, 10852–10858. doi: 10.1039/c9nr03205c

Wang, Y., Zheng, K., Song, S., Fan, D., Zhang, H., and Liu, X. (2018). Remote manipulation of upconversion luminescence. *Chem. Soc. Rev.* 47, 6473–6485. doi: 10.1039/c8cs00124c

Wu, Y., Xu, J., Poh, E. T., Liang, L., Liu, H., Wang, J. K. W., et al. (2019). Upconversion superburst with sub-2 μm lifetime. *Nat. Nanotechnol.* 14, 1110–1115. doi: 10.1038/s41565-019-0560-5

Yuan, Z., Zhang, L., Li, S., Zhang, W., Lu, M., Pan, Y., et al. (2018). Paving metal-organic frameworks with upconversion nanoparticles via self-assembly. *J. Am. Chem. Soc.* 140, 15507–15515. doi: 10.1021/jacs.8b10122

Zhang, F., and Wang, C. C. (2008). Fabrication of one-dimensional iron oxide/silica nanostructures with high magnetic sensitivity by dipole-directed self-assemble. *J. Phys. Chem. C* 112, 15151–15156. doi: 10.1021/jp804452r

Zhao, J., Chen, X., Chen, B., Luo, X., Sun, T., Zhang, W., et al. (2019). Accurate control of core-shell upconversion nanoparticles through anisotropic strain engineering. *Adv. Funct. Mater.* 29:1903295. doi: 10.1002/adfm.201903295

Zheng, K., Han, S., Zeng, X., Wu, Y., Song, S., Zhang, H., et al. (2018). Rewritable optical memory through high-registry orthogonal upconversion. *Adv. Mater.* 30:1801726. doi: 10.1002/adma.201801726

Zheng, K., Loh, K. Y., Wang, Y., Chen, Q., Fan, J., Jung, T., et al. (2019). Recent advances in upconversion nanocrystals: expanding the kaleidoscopic toolbox for emerging applications. *Nano Today* 29:100797. doi: 10.1016/nantod.2019.100797

Zhou, B., Shi, B., Jin, D., and Liu, X. (2015). Controlling upconversion nanocrystals for emerging applications. *Nat. Nanotechnol.* 10, 924–936. doi: 10.1038/nnano.2015.251

Zhou, J., Liu, Q., Feng, W., Sun, Y., and Li, F. (2015). Upconversion luminescent materials: advances and applications. *Chem. Rev.* 115, 395–465. doi: 10.1021/cr400478f

Zhou, M., Ge, X., Ke, D. M., Tang, H., Zhang, J. Z., Calvaresi, M., et al. (2019). The bioavailability, biodistribution, and toxic effects of silica-coated upconversion nanoparticles *in vivo*. *Front. Chem.* 7:218. doi: 10.3389/fchem.2019.00218

Zhu, X., Su, Q., Feng, W., and Li, F. (2017). Anti-stokes shift luminescent materials for bio-application. *Chem. Soc. Rev.* 46, 1025–1039. doi: 10.1039/c6cs00415f

**Conflict of Interest:** The authors declare that the research was conducted in the absence of any commercial or financial relationships that could be construed as a potential conflict of interest.

*Copyright © 2020 Su, Zhou, Zhou, Sun, Ai and Su. This is an open-access article distributed under the terms of the Creative Commons Attribution License (CC BY). The use, distribution or reproduction in other forums is permitted, provided the original author(s) and the copyright owner(s) are credited and that the original publication in this journal is cited, in accordance with accepted academic practice. No use, distribution or reproduction is permitted which does not comply with these terms.*